

# UNCONFINED HYDROGEN DETONATIONS: EXPERIMENTS, MODELLING, SCALING

M. Kuznetsov<sup>1\*</sup>, A. Lelyakin<sup>1</sup>, J. Xiao<sup>1</sup>, W. Breitung<sup>2</sup>, D. Banuti<sup>1</sup>

<sup>1</sup> Karlsruhe Institute of Technology, Kaiserstrasse 12, Karlsruhe 76131, Germany,

<sup>2</sup> Pro-Science GmbH, Parkstrasse 9, Ettlingen 76275, Germany

\*E-mail: [kuznetsov@kit.edu](mailto:kuznetsov@kit.edu)

## ABSTRACT

A series of unconfined hydrogen detonation bench-mark experiments are analyzed with respect to CFD code validation and safety measures development. 1-Dimensional in-house code COM1D was applied for validation against experimental data for unconfined detonation of a hemispherical envelope of about 3- and 5-m radius with hydrogen-air mixtures from 20 to 30% hydrogen in air. The code demonstrates a very good agreement with experimental data and allows an adequate simulation of the unconfined hydrogen detonation. All calculated data were scaled in Sachs coordinates to compare with experimental data and to approximate the data for practical evaluation of safety distances. Numerical experiments with different hydrogen inventories from 50 g to 50 kg and different sizes of the cloud from 1 to 2 m radius of the same amount of hydrogen 50g were carried out to clarify the problem of energy of gaseous explosion responsible for the strength of blast wave. Additionally, a comparison of hydrogen-air explosion pressure with blast wave properties from the hypothetical cloud of hot compressed combustion products ( $P=P_{icc}$ ;  $T=T_{icc}$ ) and simply a hot air of the same initial pressure and temperature as combustion products showed very good agreement of shock wave strength at far distances, beyond the cloud. This confirms the governing role of energy of combustion on blast wave propagation and its ability to scale the strength of blast waves. The dynamics of the explosion process and combustion product expansion were also analyzed experimentally and numerically to evaluate the dimension of the heat radiation zone and heat flux from combustion products. To demonstrate the capability of tested COM1D code, the modeling and analysis of high-pressure hydrogen tanks rupture at 350 and 700 bar were conducted to investigate blast wave strength and evaluate the safety distances.

## 1.0 INTRODUCTION

Hydrogen application as an energy carrier and the wide distribution of hydrogen in high technologies over the world, especially taking into account the explosivity of hydrogen being mixed with ambient air, lead to strong demand for safety measures and safety distances evaluation. The unconfined explosion of a hydrogen – air mixture or a high-pressure hydrogen tank rupture are the worst accident scenarios to be well-predicted and mitigated or avoided, if possible. Thus, the analysis of existing data and the new experimental data on high-pressure hydrogen explosions are required to develop the risk assessment, safety recommendations and user guidelines for industry and technologies.

The most known experimental data are relevant to unconfined hydrogen explosion and mostly cover the deflagration mode of flame propagation with a maximum flame speed lower than 100 m/s and a maximum combustion pressure lower than 15kPa [1-2]. To achieve the worst-case scenario, a direct initiation of detonation for hydrogen–air mixtures from 20 to 30 vol.% H<sub>2</sub> was provided by a high explosive charge in the center of a hemispherical [3,4] or a cylinder gaseous charge from 21 to 53 vol.% H<sub>2</sub> [5]. The most documented experiments [3] with respect to details of pressure measurements were used as bench-mark experiments for 3D numerical codes (DET3D, GASFLOW) validation [6-8]. Because 3D numerical simulations of hydrogen-air detonation and especially the blast wave propagation in a far zone is a time-consuming procedure, a 1D COM1D code was developed to save time without losing the quality of simulations [9]. The data of [4] and [5] have been used for scaling blast wave characteristics under unconfined hydrogen detonations. Pressure and impulse are the major integral characteristics of an explosion and depend on the energy of the process. The higher energy of the explosion leads to slower decaying strength of the blast wave. To summarize all the experimental

data on blast wave characteristics as a function of maximum pressure or impulse against the distance for different energy of exploding gas so-called dimensionless Sachs co-ordinates can be used:

- dimensionless distance: 
$$\bar{R} = x(P_0 / E)^{1/3}, \quad (1)$$

- dimensionless pressure: 
$$\bar{P}^+ = \Delta P^+ / P_0, \quad (2)$$

- dimensionless impulse: 
$$\bar{I}^+ = \Delta I^+ c_0 / P_0^{2/3} / E^{1/3} \quad (3)$$

where  $P_0 = p_a = 1$  bar is an ambient pressure;  $c_0$  is sonic velocity in air;  $E$  is energy of explosion.  $\Delta P^+$ ,  $\Delta I^+$  are the maximum over-pressure and the impulse of the positive phase of the pressure wave. The existing scaling correlations are mainly based on hydrocarbon explosion experimental data [10,11]. For instance, in such co-ordinates the dependency of dimensionless over-pressure and impulse was presented as a polynomial correlation for gaseous detonations [10]:

- over-pressure: 
$$\bar{P}^+ = 0.34/\bar{R}^{4/3} + 0.062/\bar{R}^2 + 0.033/\bar{R}^3 \quad (4)$$

- positive impulse: 
$$\bar{I}^+ = 0.0353/\bar{R}^{0.968} \quad (5)$$

As confirmed in [4] for hydrogen-air detonations in the hemispheric volume of  $V=300\text{m}^3$ , one of the most suitable correlations for hydrogen combustion is the correlations obtained for  $\text{C}_3\text{H}_8$ -air gaseous detonations in a hemispherical volume of  $134\text{ m}^3$  [11]:

- over-pressure: 
$$\bar{P}^+ = 0.46/\bar{R}^{4/3} + 0.099/\bar{R}^2 + 0.065/\bar{R}^3 \quad (6)$$

- positive impulse: 
$$\bar{I}^+ = 0.0556/\bar{R}^{0.968} \quad (7)$$

Since the data of [4] for hydrogen detonations fit well to correlations Eqs. (6)-(7), the blast wave pressure and impulse can be predicted for different hydrogen inventories and distances from the center. Of course, it is valid for distances beyond the hydrogen cloud. In the case of elongated or cylindrical clouds, such correlations can only work for aspect ratios  $L/D < 1:2$ . Taking into account the existence of the negative phase of the blast wave additional correlations [11] might be very useful for

- negative pressure: 
$$\bar{P}^- = 0.113/\bar{R}^{1.1} \quad (8)$$

- negative impulse: 
$$\bar{I}^- = 0.052/\bar{R}^{0.85} \quad (9)$$

To calculate so-called TNT equivalent the correlations for pressure characteristics under TNT explosion can be used:

- over-pressure: 
$$\bar{P}^+ = 3.53/\bar{R}^{4/3} - 5.59/\bar{R}^2 + 31.67/\bar{R}^3 \quad (10)$$

- positive impulse: 
$$\bar{I}^+ = 261/\bar{R}^{0.963} M_{\text{TNT}}^{1/3} \quad (11)$$

where  $M_{\text{TNT}}$  is the mass of TNT charge in kg. The unclear thing is the energy factor to be used for scaling of explosion characteristics because the dimensionless distance  $\bar{R}$  is proportional to the energy Eq. (1). Usually, total energy of combustion is used for scaling. For hydrogen, the value of combustion energy  $E = 120$  MJ/kg [4,5] is applied. If we know the experimental or calculated by Eqs. (1-10) explosion characteristics we can evaluate the safety distances for different damage degrees of human or structural objects using the corresponding damage diagrams for a certain object.

The main scope of the work is to analyze the existing experiments on unconfined hydrogen detonation to validate them using 1D numerical code COM1D and then, to develop scale correlations for hydrogen explosions. We also plan to specify the energy factor to be used for scale correlations. After the validation, the code will be used to calculate blast characteristics for hydrogen detonation and high-pressure hydrogen tank rupture in a wide range of hydrogen inventories from 50 g to 50 kg. With such data, we plan to evaluate safety distances and hazard potential for humans and structures under the explosion of different hydrogen inventories. The capability to evaluate fireball dimensions for hydrogen explosion is also demanded.

## 2.0 EXPERIMENTAL DETAILS

Three groups of hydrogen detonation experiments have been analyzed. A series of six tests on the detonation of hydrogen-air mixtures in a balloon was carried out at the Fraunhofer Institute of Technology, Germany [3]. The experiments to investigate the blast wave characteristics of premixed hydrogen-air mixtures were carried out in a thin-walled hemispherical polyethylene balloon with a volume of about 50 m<sup>3</sup>. A plastic balloon was initially filled with premixed hydrogen-air mixtures from 20 to 30 vol.%H<sub>2</sub>. The detonation was centrally initiated with 50 g of high-explosive charge. The pressure was measured with piezo-transducers mounted flush to the ground surface inside and outside the balloon. A high-speed camera has been used to monitor the detonation process.

The second group of detonation tests was performed using a 31 m<sup>3</sup>-volume cylindrical tent filled with hydrogen-air mixtures of 21, 28.6 and 52.9 vol. % of hydrogen [5]. The plastic tent has an aspect ratio  $H/D = 1: 1$  ( $D = 3.4$  m). A booster of high-explosive charge C-4 of 0.1 kg was exploded in the center to directly initiate the detonation. Blast wave pressures were measured at distances of 10, 18, 30, 49 and 81 m using PCB piezoelectric sensors. Then, experimental data were summarized as dependencies of normalized maximum pressure and positive pressure impulse against dimensionless distance according to Eq. (1), where characteristic energy of hydrogen mixture was taken as  $E = 120$  MJ/kg H<sub>2</sub>.

The third group of unconfined explosion experiments was conducted for 30% hydrogen detonations [4]. The large-scale tests used a hemispherical 300-m<sup>3</sup> volume covered with a thin plastic tent. Initiation was at the bottom center of the facility using a 10-g high-explosive charge for detonations of a homogeneous stoichiometric mixture 30 %H<sub>2</sub>. Measurements included blast pressure, heat flux, high-speed video, standard video, and infrared video. PCB-type blast pressure sensors in steel plates and heat flux sensors were placed along the ground surface. Similarly to the previous experiments [5], the data on pressure and impulse were summarized against dimensionless distance Eq. (1).

## 2.0 NUMERICAL MODELING

### 2.1 The model

For the numerical simulation of hydrogen detonation, a 1D CFD code COM1D was developed and described in the paper [9]. To simplify the program and to make it more quick and flexible, it was based on the following assumptions: - solution of the reactive Euler equations, i.e. neglect of molecular transportation processes such as diffusion, thermal conduction and viscosity; - no turbulence; - 1-dimensional geometry; - one global dominant reaction for the H<sub>2</sub>/O<sub>2</sub>-combustion; - temperature-dependent thermodynamic data for a reduced amount of components (H<sub>2</sub>, O<sub>2</sub>, H<sub>2</sub>O, N<sub>2</sub>); - 1<sup>st</sup> order solution procedure, numerical cell size in the present problem is 1-2 mm; - adiabatic assumption (no heat losses of gas to the solid boundary); - ideally reflecting boundary conditions at the solid interface. Cantera code and NASA data base were used for thermodynamic calculations [12]. The model is based on the following 1D Euler equations:

$$\frac{\partial \rho}{\partial t} + \frac{\partial \rho u}{\partial x} = 0 \quad (12)$$

$$\frac{\partial \rho u}{\partial t} + \frac{\partial \rho u^2}{\partial x} + \frac{\partial p}{\partial x} = 0 \quad (13)$$

$$\frac{\partial E}{\partial t} + \frac{\partial u(E + p)}{\partial x} = -\sum r_i \cdot H_i^f \cdot Q \quad (14)$$

$$\frac{\partial \rho f_i}{\partial t} + \frac{\partial \rho u f_i}{\partial x} = \mu_i \cdot r_i \cdot Q \quad (15)$$

Here  $\rho$ - density,  $u$ - velocity,  $E$ - total energy per unit volume (kinetic+thermal),  $f_i$ - a mass fraction of components,  $Q$ - reaction rate,  $r_i$ - stoichiometric coefficients (negative for reagents, positive for

products),  $H_i^f$ - enthalpy of formation,  $\mu_i$ - molecular mass. To simulate a detonation, the velocity term can be set equal to the sound speed of burned gas.

## 2.2 Validation tests

1-Dimensional in-house code COM1D was first applied for code validation against experimental data. The measured pressure curves from [3-6] were compared with COM1D calculations. Figure 1 (a,b) compares the measured and calculated pressure histories for two different positions, the one inside the  $H_2$ -air mixture ( $x = 0.75$  m) and the other outside of the balloon ( $x = 6.25$  m). The pressure signal profiles are in good quantitative agreement, especially within the hydrogen cloud. Outside the cloud, the calculated pressure wave decays slower than the experimental one, probably due to energy losses of the shock wave propagating above the solid ground. Figure 1 (c) shows a comparison of maximum over-pressure for all sensors vs. distance from the center for HBAL1 test [3] and COM1D calculations for stoichiometric hydrogen detonation in a hemisphere of  $R=2.95$ m. The figure demonstrates a very good validity of COM1D code for numerical simulations of unconfined detonation. Experimental maximum detonation over-pressure inside of the sphere is usually higher than that for calculations because of the acoustic noise of pressure sensors as well as the calculated blast wave over-pressure is overestimated against experiments probably due to neglected energy losses for shock wave propagating over the solid ground surface.

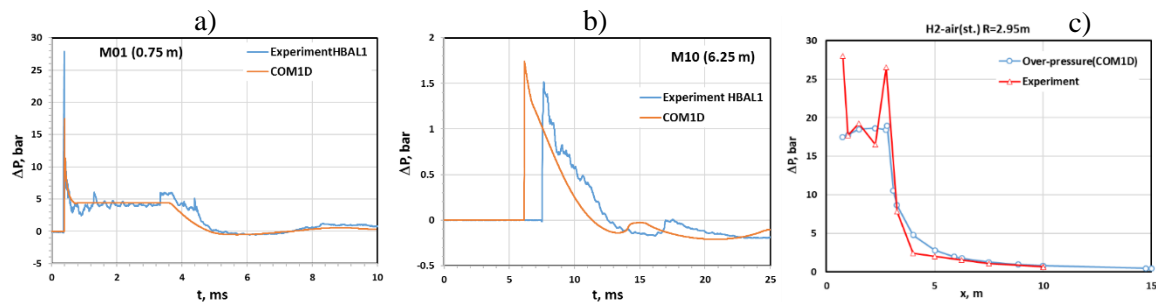


Figure 1. Comparison of pressure profiles at  $x=0.75$  m (a) and  $x=6.25$  m (b) and maximum pressure vs. distance (c) for hydrogen-air detonation experiment HBAL1 [3] and numerical simulations.

Thus, the COM1D code is able to reproduce the main features of the measured data, except that it misses weak shocks, due to the reflection from the  $H_2$ -air/air interface. Figure 2 represents so-called  $x-t$  diagrams for detonation process and further blast wave propagation as a sequence of pressure – time histories according to sensor position  $x$  from the center. The horizontal axis is the time scale  $t$ .

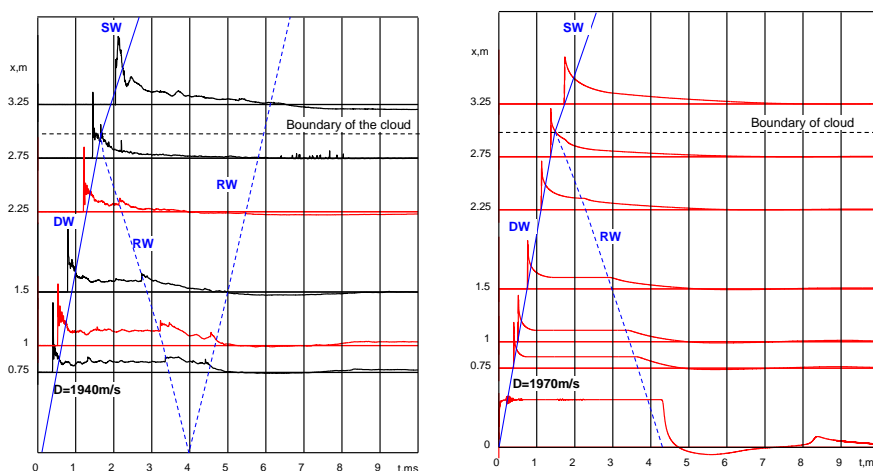


Figure 2.  $x-t$  diagram for detonation test HBAL1 [3] (left) and COM1D simulations (right): stoichiometric mixture; DW – detonation wave; SW – shock wave; RW – reflected shock wave.

The slope of the line between two characteristic peaks belonged to the local velocity of a certain process (detonations or shock propagation). As Figure 2 shows, the detonation wave (DW) propagates with a detonation velocity  $D$  until it meets the interface of hydrogen-air cloud|air. The measured and calculated detonation speeds correspond very well (1940 m/s and 1970 m/s, respectively). According to pressure measurements in experiments and calculations, the detonation reaches the end of the cloud in 1.47 ms after the ignition moment. It corresponds to 11.03 ms with a correction of 9.56 ms for the ignition moment in [3], where the detonation reaches the end between 11 and 11.2 ms. The difference might be explained by the time delay required to establish the steady state detonation after initiation using a high-explosive charge. Then, after the detonation reflection, the reflected wave (RW) propagates back through combustion products with a velocity  $u = 1165$  m/s in HBAL1 experiment and a rarefaction wave (the reflected shock was not figured out) propagates with a slower velocity of  $u = 1050$  m/s. After the hydrogen cloud is over, the detonation wave transforms to a shock wave propagating with a slower velocity  $u = 830$  m/s in the experiment and  $u = 1053$  m/s in calculations at the same distance at  $x = 3.25$  m.

A similar comparison was made for a large scale experiment with a stoichiometric hydrogen-air mixture in a 300 m<sup>3</sup> volume [4]. Figure 3 compares the measured and calculated pressure and impulse histories for sensor position outside of the balloon ( $x = 15.6$  m). The pressure signal and impulse profiles are in a good quantitative agreement but with a time shift of 2 ms, probably due to the same reason as energy losses for shock waves propagating above the solid ground. However, the maximum over-pressure and positive impulse fit very well between the experiments and simulations. The measured and calculated detonation speed also fits very well (1980 m/s and 1970 m/s, respectively). All measured maximum over-pressures and positive impulses from analyzed experiments [3-5] will be further compared with COM1D numerical simulations.

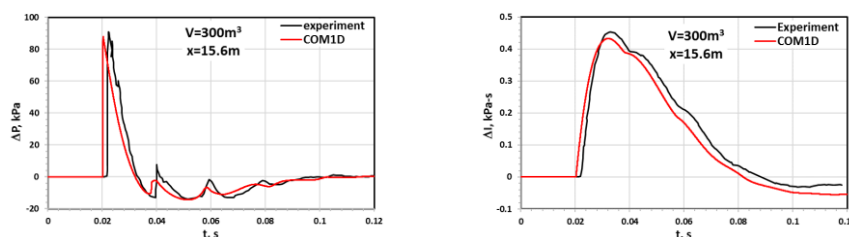


Figure 3. Comparison of pressure (left) and positive pressure impulse (right) for stoichiometric hydrogen-air detonation test [4] and COM1D simulations at sensor position  $x = 15.6$  m (right).

### 2.3 Preliminary numerical experiments ( $E = \text{const}$ , $m_{\text{H}_2} = \text{const}$ )

As confirmed, the developed COM1D code demonstrates very good agreement with experimental data and allows to extend forthcoming simulations of unconfined hydrogen detonation from 1 to 10-m radius of the cloud. Then, all calculated data will be scaled in Sachs co-ordinates to compare with experimental data [3-6] and to approximate the data for practical evaluation of safety distances.

Since all explosion characteristics (pressure and impulse) will be normalized using the energy of explosion for scaling, first series of numerical experiments will be conducted using COM1D code keeping the same energy, which is proportional to hydrogen inventory. The idea was to numerically calculate the detonation of hydrogen-air hemispheric volume of different radii from 1 to 2 m keeping the same hydrogen inventory  $m_{\text{H}_2} = 50.7$  g, which corresponds to stoichiometric hydrogen-air mixture with a radius  $R = 1$  m. Initial conditions are given in Table 1. The table gives the data on the radius of hemispherical cloud  $R$ ; initial pressure and temperature  $P_0$ ,  $T_0$ ; average hydrogen concentration %H<sub>2</sub>; theoretical Chapman-Jouguet pressure  $P_{\text{CJ}}$  and the energy of combustion  $E$  calculated by Cantera code [12]; characteristic radius  $R_0$  and impulse  $I_0$  of combustible cloud according to Eqs. (1)-(3). The numerical simulations have been conducted in an assumption of possible detonation of hydrogen – air mixtures independent of hydrogen concentration and even flammability limits.

Table 1: Initial conditions for hydrogen detonation experiment ( $m_{H_2}=50.7g$ ).

$R$ , m	$T_0$ , K	$P_0$ , bar	%H <sub>2</sub>	$P_{CJ}$ , bar	$E$ , MJ	$R_0$ , m	$I_0$ , Pa-s
1	298	1	29.59	15.6	6.08	3.93	1157
1.1	298	1	22.23	13.7	6.08	3.93	1157
1.2	298	1	17.12	11.6	6.08	3.93	1157
1.3	298	1	13.47	9.9	6.08	3.93	1157
1.4	298	1	10.78	8.5	6.08	3.93	1157
1.5	298	1	8.77	7.4	6.08	3.93	1157
2	298	1	3.70	4.2	6.08	3.93	1157

Figure 4 shows a comparison of calculated pressure and impulse for hydrogen-air detonations for the same hydrogen inventory as a function of distance from the center. For the same energy of the system, except for the cloud zone, the characteristics of the blast wave with good accuracy remain the same. This means that independent of the dimension of the detonable or suddenly expanded pressurized zone, parameters of the blast wave remain constant at the constant energy of explosion.

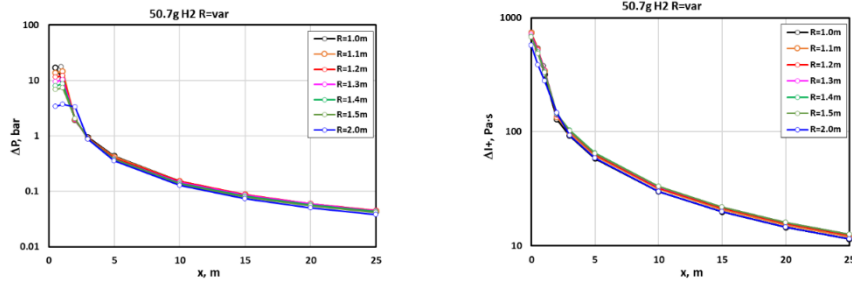


Figure 4. Comparison of pressure (left) and positive pressure impulse (right) vs distance for hydrogen-air detonation performed with COM1D numerical simulations.

A typical detonation wave profile looks like a very short detonation pressure peak roughly of  $P_{CJ}$  value and then quickly decays to a plateau at  $P_{icc}$  pressure of combustion products (see Figure 1 (a)). Since the detonation peak is very short, the main contribution to the blast energy of the shock wave gives the pressure impulse calculated as follows

$$I^+ = \int_{t_0}^{t^+} P dt \sim \Delta P^+ \Delta t^+, \quad (16)$$

which is roughly proportional to the  $P_{icc}$  overpressure times the duration of the positive pressure phase. For our curiosity, to assess the effect of the energy of combustion, we assume that the detonation very quickly, at constant volume conditions, produces a hot gas of combustion products with complete combustion pressure and temperature  $P_{icc}$  and  $T_{icc}$ , independent of the detonation velocity. Then, we consider a sudden expansion of combustion products at initial conditions  $P_{icc}$  and  $T_{icc}$  to ambient air conditions. The comparison will be done for stoichiometric hydrogen-air detonation in a hemispheric volume of  $R=1$  m (Table 2). Another comparison will be done with inert gas as air at the same initial conditions as combustion products in a constant volume combustion  $P_{icc}$  and  $T_{icc}$  (Table 2). Here we assume that the physical energy of hot compressed air is similar to the energy of combustion products. Actually, the physical energy calculated for adiabatic expansion and cooling of compressed hot gas

$$W = \int_{V_1}^{V_2} P_1 \left( \frac{V_1}{V} \right)^\gamma dV = P_1 V_1^\gamma \frac{V_2^{1-\gamma} - V_1^{1-\gamma}}{1-\gamma} \quad (17)$$

is equal to 5.976 MJ, which is very close to the combustion energy of 6.08 MJ.

Table 2: Initial conditions for gases energetically equivalent to stoichiometric hydrogen-air mixture.

$R$ , m	$T_0$ , K	$P_0$ , bar	%H <sub>2</sub>	$E$ , MJ	$R_0$ , m	$I_0$ , Pa-s
1	298	1	29.59	6.08	3.93	1157
1	2752	8.023	comb. prod.	6.08	3.93	1157
1	2752	8.023	air	5.98		

Surprisingly, it follows from COM1D calculations that the integral blast wave characteristics of equivalent gases, out of the cloud, are practically identical to that for hydrogen-air detonations of the same initial volume. The only small difference occurs due to an extra energy of pressure impulse produced by the detonation peak, which was neglected in our assumption. This means that the energetic equivalent plays a governing role in blast wave propagation under a sudden expansion of combustible gas explosion or simply an expansion of pressurized gas volume.

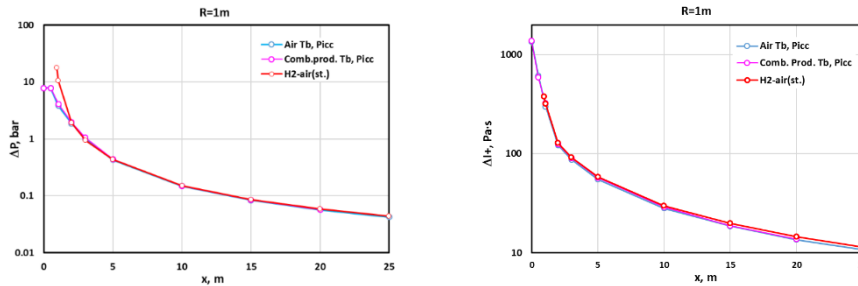


Figure 5. Comparison of pressure (left) and positive pressure impulse (right) vs distance for hydrogen-air detonation performed with COM1D numerical simulations.

### 3.0 MAIN RESULTS AND DISCUSSION

#### 3.1 Scaling tests

A series of detonation tests for stoichiometric hydrogen-air in a hemispheric volume of different radii from 1 to 10 m and a hydrogen inventory from 0.05 to 50.68 kg at ambient pressure and temperature was numerically conducted using validated COM1D code (Table 3). Validation tests for experimental data [3,4] are also included in this test series. Figure 6 shows the dependence of calculated blast wave characteristics vs distance under hydrogen-air detonation in an unconfined hemispheric volume.

Table 3: Initial conditions for stoichiometric hydrogen-air detonations ( $R = \text{var}$ ).

$R$ , m	$V$ , m <sup>3</sup>	$T_0$ , K	$P_0$ , bar	$m_{\text{H}_2}$ , g	%H <sub>2</sub>	$E$ , MJ	$R_0$ , m	$I_0$ , Pa-s
1.0	2.09	298	1	50.7	29.6	6.08	3.93	1156
2.0	16.7	298	1	405.5	29.6	48.6	7.86	2313
2.95	53.8	298	1	1301	29.6	156.1	11.6	3412
5.0	262	298	1	6336	29.6	760	19.7	5783
5.23	300	298	1	7362	30.0	883	20.7	6080
10.0	2094	298	1	50684	29.6	6082	39.3	11566

All calculated data can be normalized using the energy of combustion  $E$  as a scaling parameter. Figure 7 shows a summary of calculated and experimental data in Sachs coordinates according to Eq. (1)-(3). It shows an excellent fit between all data not only for hydrogen detonation [3-6] but also for propane-air detonation in a 134 m<sup>3</sup> hemisphere [11]. Then, we can apply for the scaling of hydrogen detonation the same correlations, obtained for propane-air detonations: Eq. (6) for maximum overpressure and Eq. (7) for positive pressure impulse. The validity domain for over-pressure can be extended to

$0.3 < R^* = x/R_0 < 10$  and for positive impulse  $0.4 < R^* = x/R_0 < 10$ . The correlations for propane from [11] for negative pressure Eq. (8) and impulse Eq. (9) are not as good for hydrogen as for propane (see Figure 8). Thus, we recommend the following modified correlations with their validity domains for

- negative pressure: 
$$|\bar{P}^-| = 0.11 \bar{R}^{1.02} \quad (0.47 < R^* < 10) \quad (18)$$

- negative impulse: 
$$|\bar{I}^-| = |\Delta I^- / I_0| = 0.063 \bar{R}^{0.95} \quad (0.47 < R^* < 10) \quad (19)$$

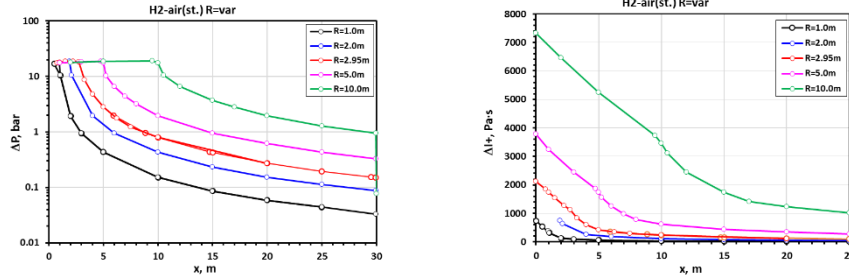


Figure 6. Dependence of calculated blast wave characteristics against distance under hydrogen-air detonation in a hemispheric volume performed with COM1D numerical simulations.

All proposed scale correlations Eq. (6)-(7), (18)-(19) work well beyond the cloud. Within the cloud ( $0 < R^* < 0.24$ ) we can recommend the next scale correlations for pressure and impulse

- the positive impulse: 
$$\bar{I}^+ = \Delta I^+ / I_0 = 0.23 \bar{R}^{0.3} \quad (0 < R^* < 0.24) \quad (20)$$

- the negative pressure: 
$$|\bar{P}^-| = |\Delta P^- / P_0| = 0.15 \bar{R}^{0.46} \quad (0 < R^* < 0.47) \quad (21)$$

- the negative impulse: 
$$|\bar{I}^-| = |\Delta I^- / I_0| = 0.11 \bar{R}^{0.15} \quad (0 < R^* < 0.47) \quad (22)$$

The level of maximum over-pressure within the cloud is equal to Chapman-Jouguet pressure  $P_{CJ}$ .

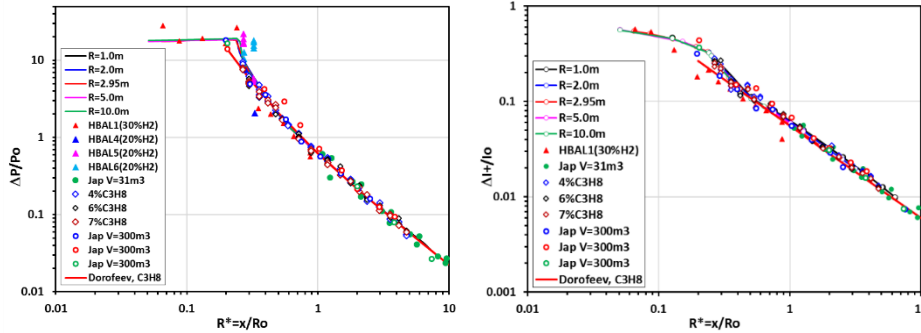


Figure 7. Dependence of dimensionless pressure and positive impulse against normalized distance for calculated and experimental data on detonation of different mixtures.

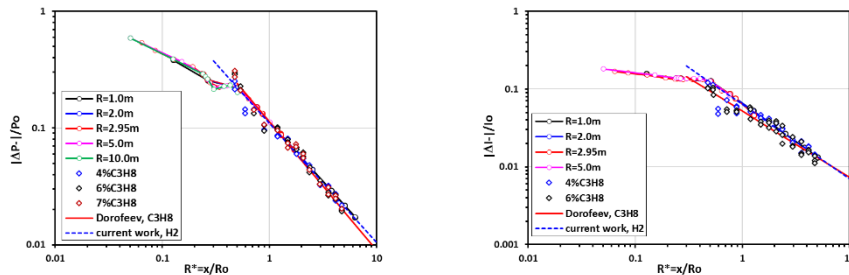


Figure 8. Dependence of dimensionless negative pressure and negative impulse against normalized distance for calculated and experimental data on detonation of different mixtures.



### 3.2 Fire ball dimension

As the high-speed video in [3,6] shows, the hot gas of combustion products expands behind the leading shock wave with the formation of a fireball. The same behaviour we can see as a result of numerical simulations (Figure 9). After the detonation wave reaches the boundary of the cloud, the flame front delays behind the leading shock wave. The temperature of the flame front very quickly reduces from 3400 K within the cloud to 2000 K at the distance  $1.5R_0$  from the center. The maximum expansion of combustion products reaches the distance  $\sim 2R_0$ . It allows evaluating the maximum dimension of radiating zone as a radius of hot products at the temperature threshold  $T=1000$  or  $T=1500$ K. One can identify it as a maximum fireball radius  $R_{FB}(1500\text{K})$  or  $R_{FB}(1000\text{K})$ . Figure 10 summarizes the data on fireball radius for hemispheric geometry, evaluated by COM1D simulations, as a function of hydrogen inventory together with experimental data of Zabetakis [13] for liquid hydrogen and data of detonation experiments in hemispherical volume from 2.1 to 134 m<sup>3</sup> for stoichiometric propane-air mixture [11] and detonation of gasoline, kerosene and diesel fuel clouds up to 100 tons of fuel [14]. To approximate the calculation data, we used so called sigma approach, where the expansion ratio  $\sigma = \rho_u/\rho_b$  is the ratio of densities unburned to burned gas. According to the thermodynamic database [12],  $\sigma = 6.89$  for stoichiometric hydrogen-air at  $P_0=1$  bar and  $T_0=298\text{K}$ . Since the volume of combustion products  $V_p = \sigma V_0$  is sigma times larger than the initial one, without dynamics of expanded combustion products, the fireball radius can be calculated as follows

- for hemispherical fireball:  $R_{hs} = 4.98m^{0.33}$  (23)

- for spherical fireball:  $R_{sp} = 3.97m^{0.33}$  (24)

The best fit of calculated data was found for the correlation Eq. (23).

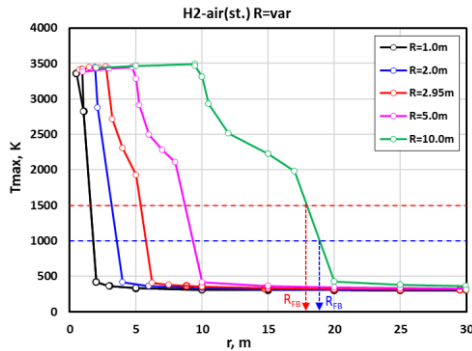


Figure 9. Dependence of temperature of the cloud against distance from the cloud.

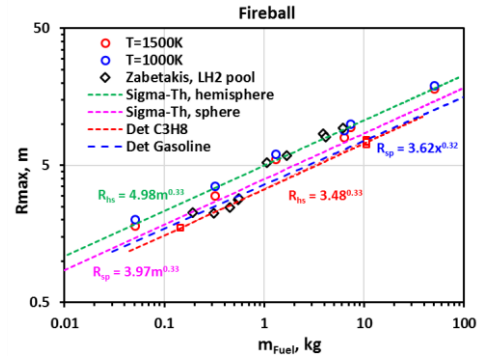


Figure 10. Dimension of maximum fireball radius as a function of mass of the fuel.

The maximum heat flux from hydrogen-air detonation was measured in [4] at two different distances that give a value at the flame ball surface  $q_{max} = 160 \text{ kW/m}^2$ . Assuming two times lower average heat flux  $q_{av}=80\text{kW/m}^2$  than the maximum during the characteristic time of flameball under detonation [14]

$$t_D = 0.15m^{0.33} \quad (25)$$

one can evaluate the emissivity factor of radiative heat flux  $\varepsilon = E_{rad}/E_0 = 0.056$  as a small fraction of the total energy of combustion. With known heat flux at the surface and characteristic time of heat radiation, the safety distances can be evaluated for different hazard degrees.

### 3.3 High pressure tank rupture

After validation tests, four cases of high pressure hydrogen storage tank rupture were simulated with COM1D code for four hemispherical volumes of pressurized hydrogen (Table 4). Initial conditions are given in Table 4 together with the energy of the system in different assumptions [15-18].

Table 4: Initial conditions for high-pressure tank rupture ( $m_{H_2}$ ,  $P_0 = \text{var}$ ).

$R$ , m	$V$ , m <sup>3</sup>	$m_{H_2}$ , kg	$T$ , K	$P$ , bar	$E$ , MJ			$m_{TNT}$ , kg
					Adiabatic (Brode, 1959)	Isentropic (Smith, 1987)	Crowl, 1992	
0.25	0.0327	0.763	298	350	2.85	2.33	5.57	0.4
0.5	0.262	6.104	298	350	22.84	18.61	44.54	3.5
0.25	0.0327	1.284	298	700	5.72	4.85	12.72	0.8
0.5	0.262	10.27	298	700	45.75	38.77	101.8	6.0

Figure 11 shows the dependences of calculated blast wave characteristics against distance from the center for different high pressure tanks (350 and 700 bar) with different hydrogen inventories from 0.76 to 10.27 kg H<sub>2</sub>. For scaling analysis, all the data can be collapsed to one line using Sachs coordinates, Eq. (1)-(3). The problem is to choose the proper energy of the explosion (Table 5). Since the energy of the explosion is proportional to the mass of pressurized hydrogen one can operate in terms of mass  $m_{H_2}$  to normalize the variables (Figure 12). Such a form also allows to compare numerical simulations with experiments for 72.4 and 150 litres of hydrogen pressurized to 343 and 500 bar [19-21]. Unpublished report [21] gives the over-pressure level of 1.16, 1.46, 0.847, 0.7 at 5 m from the epicenter for four directions under the burst of 150 litre type III cylinder of 500 bar H<sub>2</sub>. The figure demonstrates very good agreement between experiments and calculations.

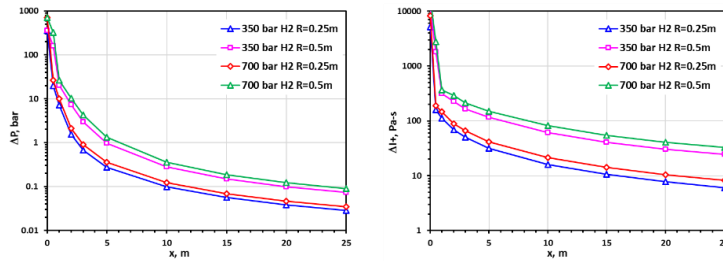


Figure 11. Dependence of calculated blast wave characteristics against distance under high pressure hydrogen tank rupture in a hemispherical volume performed with COM1D numerical simulations.

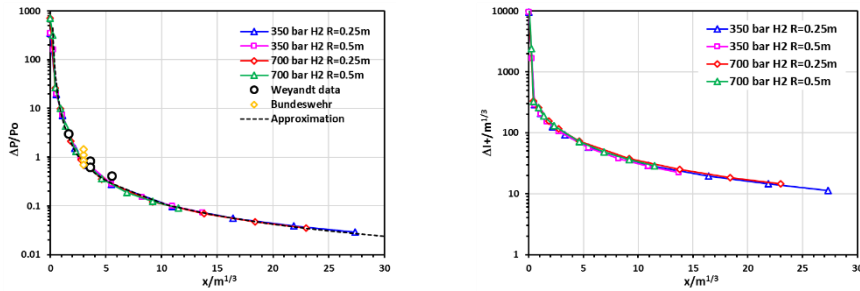


Figure 12. Calculated normalized blast wave characteristics against distance under high pressure hydrogen tank rupture compared with experiments [19-21].

Finally, a comparison of blast characteristics for high-pressure tank rupture with hydrogen/air explosion (Figure 13) allows to define an energetic equivalent of high-pressure tank rupture. For 350 bar tank rupture, the energy  $E = 21$  MJ corresponds to 175 g hydrogen detonation, and for 700 bar tank rupture, the energy  $E = 48.65$  MJ corresponds to 2 kg hydrogen detonation. Both values are closer to the adiabatic assumption [15,16] for the internal energy of pressurized hydrogen (Table 5). Another measure of explosion energy can be a TNT equivalent (Table 5) calculated using Eq. (10) for pressure.

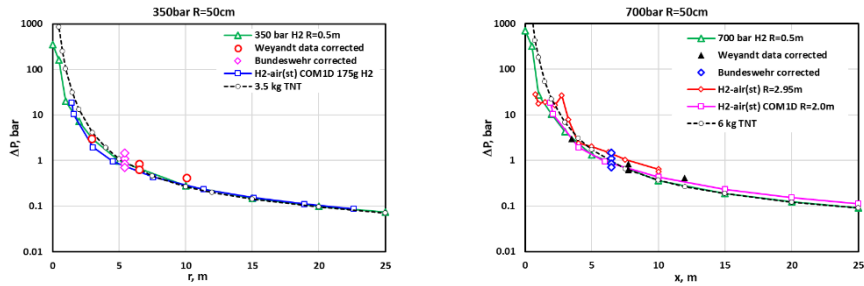


Figure 13. Calculated normalized blast wave characteristics against distance under high pressure hydrogen tank rupture compared with experiments [19-21].

### 3.4 Safety distance evaluation

The real strength of a blast wave from hydrogen detonation or high-pressure tank rupture can be estimated as a pressure – impulse effect on real objects. The hazard potential of an explosion can be evaluated against a human or a structural object. Figure 14 shows so called *P-I* pressure – impulse diagrams for human and structural objects taken from [22-24]. Several curves above the diagram show blast characteristics of hydrogen explosions from 50 g to 50 kg at different distances. The distances below a certain damage degree define the safe position. As the Figure shows, the blast of high-pressure tanks at 350 and 700 bar with 6 and 10 kg H<sub>2</sub> leads to the same harm as the detonation of 50 to 400 g H<sub>2</sub>. One can see that the duration of the pressure impulse plays an important role in the object response. For instance, for 1.3 kg H<sub>2</sub> detonation, the safety distances for damage of structural objects with respect to impulse are 2-2.5 times shorter than against the pressure (Table 5). For human objects, the impulse response 1.5 times shortens the safety distance. The eardrum rupture threshold is assumed as the weakest for humans and the criterion of 50% of windows broken for structural objects. The 50% fatality for humans and full buildings demolition for structures are assumed as the strongest harm degree. The most conservative impulse-based safety distance (if possible) should be taken for safety analysis and risk assessment.

Table 5: Safety distances under hydrogen detonations.

Hydrogen inventory, kg	0.051	0.41	1.3	6.34	50.7
Humans					
Impulse-based					
50% fatality probability	4.0	8.7	14.2	29.0	63
People are knocked down	1.6	4.0	5.8	11.5	28
Pressure-based					
Eardrum rupture threshold	11.0	22.0	32.5	55.0	110
90% eardrum rupture probability	2.8	5.5	8.2	13.8	28
50% fatality probability	1.8	5.9	9.8	20.1	53
People are knocked down	0.4	1.1	3.0	4.5	15
Structures					
Impulse-based					
Minor structural damage	3.8	13	26	70	266
Full demolition, 100% of walls destroyed	1.5	3.8	6.9	16	54
Pressure-based					
50% of window frame broken	35	71	105	177	355
Complete window/glass broken	18	35	52	88	175
Minor structural damage	22	44	65	110	221
Full demolition, 100% of walls destroyed	5.3	11	16	27	53

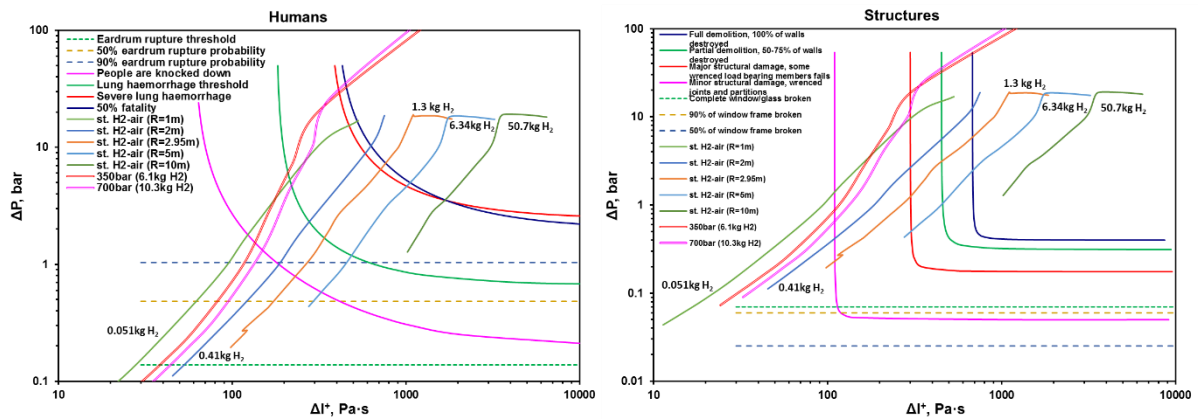


Figure 14. Damage diagrams for human and structural objects with respect to hydrogen detonations and high-pressure tank rupture.

#### 4.0 SUMMARY AND CONCLUSIONS

1-Dimensional in-house code COM1D was successfully applied for validation against experimental data for the unconfined detonation of a hemispherical envelope of about 3- and 5-m radius with hydrogen-air mixtures from 20 to 30% hydrogen in air. Numerical experiments with different hydrogen inventories from 50 g to 50 kg and different sizes of the cloud from 1 to 2 m radius of the same amount of hydrogen 50g were carried out to clarify the problem of energy of gaseous explosion responsible for the strength of blast wave. Additionally, a comparison of hydrogen-air explosion pressure with blast wave properties from the hypothetical cloud of hot compressed combustion products ( $P=P_{icc}$ ;  $T=T_{icc}$ ) and a hot air cloud of the same initial pressure and temperature as combustion products showed very good agreement of shock wave strength at far distances, beyond the cloud. This also confirms the governing role of the energy of combustion on blast wave propagation and the ability to scale the strength of blast wave using the energy of combustion as a scaling parameter. All calculated data were scaled in Sachs coordinates to compare with experimental data and to approximate the data for practical evaluation of safety distances. The dynamics of the explosion process and combustion product expansion were numerically analyzed to evaluate the radius of the heat radiation zone and heat flux from combustion products. To demonstrate the capability of tested COM1D code, the modeling and analysis of high-pressure hydrogen tank rupture at 350 and 700 bar has been conducted to investigate the blast wave propagation and to evaluate the safety distances. It was shown that the most conservative safety distance based on critical impulse evaluation should be taken for the safety analysis.

#### REFERENCES

1. Schneider H, Pfortner H. PNP-Sicherheitsfortprogramm, Prozeßgasfreisetzung-Explosion in der Gasfabrik und Auswirkungen von Druckwellen auf das Containment. Dezember 1983.
2. Becker T, Ebert F, (1985) Vergleich zwischen Experiment und Theorie der Explosion grober, freier Gaswolken. *Chem.-Ing.-Tech.*, 57(1) : 42-45.
3. Pfortner H, (1991) Ausbreitungsfunktionen detonierender Wasserstoff-Luft Gemische, Report FhG-Projekt Nr. 102555, Fraunhofer-Institut für Chemische Technologie, Pfinztal-Berghausen, Germany (Dec. 1991).
4. M. Groethe, E. Merilo, J. Colton, S. Chiba, Y. Sato, H. Iwabuchi (2007) Large-scale hydrogen deflagrations and detonations, *International Journal of Hydrogen Energy*, 32(13) : 2125-2133.
5. K. Wakabayashi, T. Mogi, D. Kim, T. Abe, K. Ishikawa, E. Kuroda, T. Matsumura, Y. Nakayama, S. Horiguchi, M. Oya (2005) A Field Explosion Test of Hydrogen-Air Mixtures. Proc. ICHS2005, paper #39, pp. 1-12.

6. W. Breitung, R. Redlinger, P. Roysl (1994) Untersuchungen zur Verteilung und Verbrennung von Wasserstoff in DWR-Anlagen. Statusbericht des Projektes Nukleare Sicherheitsforschung (PSF), KfK 5326, Mai 1994, pp. 167-214
7. Xiao, J., Breitung, W., Kuznetsov, M., Travis, J. R., Redlinger, R. (2017). Development and validation of the parallel all-speed CFD code GASFLOW-MPI for detonation of premixed H<sub>2</sub>-air mixture in a hemispherical balloon. Proc. of the 25th International Conference on Nuclear Engineering, ICONE25-66066.
8. D. Kim & J. Kim (2019) Numerical method to simulate detonative combustion of hydrogen-air mixture in a containment, *Engineering Applications of Computational Fluid Mechanics*, 13(1): 938-953
9. M. Kuznetsov, A. Lelyakin, W. Breitung (2010). Numerical Simulation of Radiolysis Gas Detonations in a BWR Exhaust Pipe and Mechanical Response of the Piping to the Detonation Pressure Loads. In: Numerical Simulations - Examples and Applications in Computational Fluid Dynamics, Lutz Angermann (Ed.), pp 389-412. ISBN: 978-953-307-153-4, InTech Publishers, Rijeka, Croatia, DOI: <http://dx.doi.org/10.5772/12839>.
10. Dorofeev S.B. (1995) Blast effects of confined and unconfined explosions, Proc. of 20th Symp. (Int.) on *Shock Waves*, Pasadena, CA, USA, July 1995, pp. 77 – 86
11. Dorofeev, S.B., Sidorov V.P., Kuznetsov M.S., Dvoishnikov A.E., Alekseev V.I., Efimenko A.A. (1996) Air blast and heat radiation from fuel-rich mixture detonation. *Shock Waves*, 6: 21-28.
12. Goodwin, D.G., Speth, R.L., Moffat, H.K., and Weber, B.W. (2021) Cantera: An Object-oriented Software Toolkit for Chemical Kinetics, Thermodynamics, and Transport Processes, Version 2.5
13. Zabetakis, M. G. (1965) Flammability characteristics of combustible gases and vapors. Bureau of Mines Bulletin 627. Pittsburgh.
14. S.B. Dorofeev, V.P. Sidorov, A.A. Efimenko, A.S. Kochurko, M.S. Kuznetsov, B.B. Chaivanov, D.I. Matsukov, A.K. Pereverzev, V.A. Avenyan (1995) Fireballs from deflagration and detonation of heterogeneous fuel-rich clouds, *Fire Safety Journal*, Volume 25, Issue 4, Pages 323-336.
15. Brode H.L. (1959) Blast waves from a spherical charge. *Phys Fluids*, 2:217-29.
16. Zel'dovich, Ya.B. and Kompaneets, A.S. (1955) Theory of Detonation, Gostekhizdat, Moscow, 268 p.
17. Smith, J.M, Van Ness, H.C. (1987) Introduction to chemical engineering thermodynamics. 4th ed. New York: McGraw-Hill.
18. Crowl D.A. (1992) Calculating the energy of explosion using thermodynamic availability. *J Loss Prev Process Ind*; 5(2):109-18.
19. Weyandt N. (2005) Analysis of induced catastrophic failure of a 5000 psig type IV hydrogen cylinder. Southwest Research Institute Report for the Motor Vehicle Fire Research Institute; 01.06939.01.001.
20. Weyandt N. (2006) Vehicle bonfire to induce catastrophic failure of a 5000-psig hydrogen cylinder installed on a typical SUV. Southwest Research Institute Report for the Motor Vehicle Fire Research Institute.
21. Heymann A.F. (2012) Auswertung Mobile Notversorgung Wasserstoff Druckverlaufsmessung, Versuch 15 vom 08.11.2012. Bundeswehr, Projektnr.: R1/0000009704-28
22. Mannan S. (2005) Lees' loss prevention in the process industries. 3rd ed., Vol. 1. Elsevier Butterworth-Heinemann.
23. Molkov, V., Kashkarov, S. (2015) Blast wave from a high-pressure gas tank rupture in a fire: Stand-alone and under-vehicle hydrogen tanks, *International Journal of Hydrogen Energy*, 40 (36): 12581-12603.
24. Kuznetsov, M., Yanez, J., Grune, J., Friedrich, A., Jordan, T., (2015) Hydrogen combustion in a flat semi-confined layer with respect to the Fukushima Daiichi accident, *Nuclear Engineering and Design*, 286 : 36-48